THE JOURNAL OF BIOLOGICAL CHEMISTRY
Vol. 276, No. 26, Issue of June 29, pp. 23903–23913, 2001
Printed in U.S.A.

Endogenous Formation of Protein Adducts with Carcinogenic Aldehydes

IMPLICATIONS FOR OXIDATIVE STRESS*

Received for publication, March 5, 2001, and in revised form, March 19, 2001
Published, JBC Papers in Press, March 30, 2001, DOI 10.1074/jbc.M101947200

Kanako Ichihashi‡, Toshihiko Osawa‡, Shinya Toyokuni§, and Koji Uchida‡¶

From the ‡Laboratory of Food and Biodynamics, Graduate School of Bioagricultural Sciences, Nagoya University, Nagoya 464-8601 and the §Department of Pathology and Biology of Diseases, Graduate School of Medicine, Kyoto University, Sakyo-ku, Kyoto 606, Japan

In the present study, we characterize the covalent modification of a protein by crotonaldehyde, a representative carcinogenic aldehyde, and describe the endogenous production of this aldehyde *in vivo*. The crotonaldehyde preferentially reacted with the lysine and histidine residues of bovine serum albumin and generated a protein-linked carbonyl derivative. Upon incubation with the histidine and lysine derivatives, crotonaldehyde predominantly generated β-substituted butanal adducts of histidine and lysine and N^{ϵ}-(2,5-dimethyl-3-formyl-3,4-dehydropiperidino)lysine (dimethyl-FDP-lysine) as the putative carbonyl derivatives generated in the crotonaldehyde-modified protein. To verify the endogenous formation of crotonaldehyde *in vivo*, we raised the monoclonal antibody (mAb82D3) against the crotonaldehyde-modified protein and found that it cross-reacted with the protein-bound 2-alkenals, such as crotonaldehyde, 2-pentenal, and 2-hexenal. The anti-2-alkenal antibody recognized multiple crotonaldehyde-lysine adducts, including dimethyl-FDP-lysine and an unknown product, which showed the greatest immunoreactivity with the antibody. On the basis of the chemical and spectroscopic evidence, the major antigenic product was determined to be a novel Schiff base-derived crotonaldehyde-lysine adduct, N^{ϵ}-(5-ethyl-2-methylpyridinium)lysine (EMP-lysine). It was found that the lysine residues that had disappeared in the protein treated with crotonaldehyde were partially recovered by EMP-lysine. The presence of immunoreactive materials with mAb82D3 *in vivo* was demonstrated in the kidney of rats exposed to the renal carcinogen, ferric nitrilotriacetate. In addition, the observations that the metal-catalyzed oxidation of polyunsaturated fatty acids in the presence of proteins resulted in an increase in the antigenicity of the protein indicated that lipid peroxidation represents a potential pathway for the formation of crotonaldehyde/2-alkenals *in vivo*. These data suggest that the formation of carcinogenic aldehydes during lipid peroxidation may be causally involved in the pathophysiological effects associated with oxidative stress.

Several lines of evidence indicate that the oxidative modification of protein and the subsequent accumulation of the modified proteins have been found in cells during aging, oxidative stress, and in various pathological states, including premature diseases, muscular dystrophy, rheumatoid arthritis, and atherosclerosis (1–4). The important agents that give rise to the modification of a protein may be represented by reactive aldehydic intermediates, such as ketoaldehydes, 2-alkenals and 4-hydroxy-2-alkenals (3, 5, 6). These reactive aldehydes are considered important mediators of cell damage due to their ability to covalently modify biomolecules, which can disrupt important cellular functions and can cause mutations (5). Furthermore, the adduction of aldehydes to apolipoprotein B in low density lipoproteins (LDL)[1] has been strongly implicated in the mechanism by which LDL is converted to an atherogenic form that is taken up by macrophages, leading to the formation of foam cells (7, 8).

2-Alkenals represent a group of highly reactive aldehydes containing two electrophilic reaction center (Fig. 1). A partially positive carbon 1 or 3 in such molecules can attack a nucleophile, such as protein. It has been suggested that these aldehydes primarily react with the sulfhydryl group of cysteine, the ε-amino group of lysine, and the imidazole group of histidine in the proteins (5, 6). Among the 2-alkenals, crotonaldehyde is known to be mutagenic in *Salmonella typhimurium* and other systems used for the detection of genetic damage (9). Its high reactivity indeed makes this aldehyde a dangerous substance for the living cell. It has been shown that crotonaldehyde induces altered liver cell foci, neoplastic nodules, and hepatocellular carcinoma upon oral administration to F344 rats (9, 10). Crotonaldehyde is commonly detected in mobile source emissions, cigarette smoke, and other products of thermal degradation (9). It is also a product of lipid peroxidation and a metabolite of the hepatocarcinogen *N*-nitrosopyrrolidone and forms adducts with DNA (11–14). Crotonaldehyde, like other 2-alkenals, may also form adducts with the nucleophilic amino acid residues of protein; however, there have been few detailed insights into the chemical mechanism involved in the modification of proteins by crotonaldehyde.

To understand the mechanism underlying the formation of covalently modified protein *in vivo*, we have initiated studies

[1] The abbreviations used are: LDL, low density lipoprotein; dimethyl-FDP-lysine, N^{ϵ}-(2,5-dimethyl-3-formyl-3,4-dehydropiperidino)lysine; FDP-lysine, N^{ϵ}-(3-formyl-3,4-dehydropiperidino)lysine; EMP-lysine, N^{ϵ}-(5-ethyl-2-methylpyridinium)lysine; ELISA, enzyme-linked immunosorbent assay; HMBC, ^{1}H-detected multiple-bond heteronuclear multiple quantum coherence spectrum; Fe^{3+}-NTA, ferric nitrilotriacetate; KLH, keyhole limpet hemocyanin; DNPH, 2,4-dinitrophenylhydrazine; BSA, bovine serum albumin; LC-MS, liquid chromatography-mass spectrometry; mAb, monoclonal antibody; HPLC, high performance liquid chromatography; PAGE, polyacrylamide gel electrophoresis.

* The costs of publication of this article were defrayed in part by the payment of page charges. This article must therefore be hereby marked "*advertisement*" in accordance with 18 U.S.C. Section 1734 solely to indicate this fact.

¶ To whom correspondence should be addressed: Laboratory of Food and Biodynamics, Graduate School of Bioagricultural Sciences, Nagoya University, Nagoya 464-8601, Japan. Tel.: 81-52-789-4127; Fax: 81-52-789-5741; E-mail: uchidak@agr.nagoya-u.ac.jp.

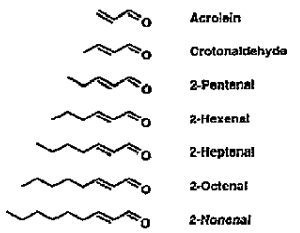

FIG. 1. **Chemical structures of 2-alkenals.**

on the characterization of modified proteins with reactive aldehyde species. In the present study, we investigated the reaction of protein with crotonaldehyde and determined the structures of the crotonaldehyde adducts, possessing a carbonyl function. Moreover, to assess their formations *in vivo*, we raised the monoclonal antibody directed to protein-bound crotonaldehyde and examined the endogenous production of antigenic materials in an experimental carcinogenesis model. Our results suggest that crotonaldehyde/2-alkenals and their protein adducts are endogenously produced under oxidative stress. Finally, lipid peroxidation is demonstrated to be a potential pathway for the endogenous formation of 2-alkenals.

EXPERIMENTAL PROCEDURES

Materials

N^{α}-Hippuryl-L-lysine, N^{α}-acetyl-L-histidine, crotonaldehyde, and bovine serum albumin (BSA) were obtained from Sigma Chemical Co. Keyhole limpet hemocyanin (KLH) was obtained from Pierce. Ferric nitrate nonahydrate and sodium carbonate were from Wako (Osaka, Japan); and the nitrilotriacetic acid disodium salt was from Nacalai Tesque, Inc. (Kyoto, Japan). Horseradish peroxidase-linked anti-rabbit IgG immunoglobulin and ECL (enhanced chemiluminescence). Western blotting detection reagents were obtained from Amersham Pharmacia Biotech.

General Procedures

NMR spectra were recorded using a Bruker AMX600 (600 MHz) instrument. Ultraviolet absorption spectra were measured with a Hitachi U-Best-50 spectrophotometer, and fluorescence spectra were recorded with a Hitachi F-2000 spectrometer. Fast atom bombardment-mass spectrometry was measured with a JEOL JMS-700 (MStation) instrument. Liquid chromatography-mass spectrometry (LC-MS) was measured with a Jasco PlatformII-LC instrument.

In Vitro Modification of BSA

Modification of the protein by crotonaldehyde was performed by incubating BSA (1.0 mg/ml) with 1–10 mM crotonaldehyde in 10 ml of 0.1 M sodium phosphate buffer (pH 7.2) at 37 °C for 24 h. The iron-catalyzed oxidation of arachidonate in the presence of BSA was performed by incubating BSA (1 mg/ml) with 2 mM polyunsaturated fatty acids in the presence of either 10 μM Fe^{2+}, 1 mM ascorbate, or 10 μM Fe^{2+} and 1 mM ascorbate in 0.1 ml of 0.1 M sodium phosphate buffer (pH 7.4) in atmospheric oxygen.

Reaction of Amino Acid Derivatives with Crotonaldehyde

Crotonaldehyde-N^{α}-acetylhistidine—The reaction mixture (10 ml) contained 100 mM crotonaldehyde and 100 mM N^{α}-acetylhistidine in 50 mM sodium phosphate buffer (pH 7.2). After incubation for 48 h at 37 °C, the reaction mixtures were analyzed with a reverse-phase HPLC using a Develosil ODS-HG-5 column (4.6 × 250 mm, Nomura Chemicals, Aichi, Japan) equilibrated in 0.1% trifluoroacetic acid at a flow rate of 0.8 ml/min. The elution profiles were monitored by absorbance at 200–400 nm. The reaction gave a single product, which was isolated (yield, 18 mg) with a reverse-phase HPLC using a Develosil ODS-HG-5 column (20.0 × 250 mm, Nomura Chemicals) equilibrated in 0.1% trifluoroacetic acid at a flow rate of 8.0 ml/min. The chemical structure of the product was characterized by LC-MS and ^{1}H and ^{13}C NMR spectrometries. ^{1}H NMR (CD3OD): δH 1.46 (^{3}H, d, J = 6.76 Hz), 1.81 (^{3}H, s), 2.91 (1H, m), 3.09 (1H, m), 3.10 (2H, m), 4.53 (1H, m), 4.95 (1H, m), 7.59, (1H, s), 8.24 (1H, d, J = 8.12 Hz), 9.07 (1H, s), 9.58 (1H, s); δC 20.78, 22.27, 26.72, 48.38, 50.39, 50.94, 117.76, 130.31, 134.1, 169.34, 171.98, 200.13.

Crotonaldehyde-N^{α}-hippuryllysine—The reaction mixture (10 ml) contained 100 mM crotonaldehyde and 100 mM N^{α}-hippuryllysine in 50 mM sodium phosphate buffer (pH 7.2). After incubation for 24 h at 37 °C, the reaction mixtures were analyzed with a reverse-phase HPLC using a Develosil ODS-MG-5 column (4.6 × 250 mm, Nomura Chemicals) equilibrated in a solution of 20% methanol in 0.1% acetic acid at a flow rate of 0.8 ml/min. The elution profiles were monitored by absorbance at 240 nm. The reaction provided two major products (P-1 and P-2), but only P-2 was isolable (yield, 12 mg). P-2 was isolated with a reverse-phase HPLC using a Develosil ODS-HG-5 column (20.0 × 250 mm) equilibrated in 23% methanol in 0.1% acetic acid at a flow rate of 6.0 ml/min. The molecular masses of P-1 and P-2 were estimated by LC-MS. The chemical structure of P-2 was characterized by ^{1}H and ^{13}C NMR spectrometries. ^{1}H NMR (CD3OD): δH 1.13 (2H, m), 1.19 (^{3}H, m), 1.29 (^{3}H, d, J = 6.76 Hz), 1.49–1.67 (4H, m), 2.25–2.50 (2H, m), 2.95 (2H, m), 3.75 (1H, m), 3.88 (2H, m), 4.08 (1H, m), 4.21 (1H, q, J = 7.62 Hz), 6.95 (1H, m), 7.33 (2H, t, J = 7.40, 8.04 Hz), 7.43 (1H, m), 7.60 (2H, d, J = 7.32 Hz), 9.10 (1/2 H, s), 9.16 (1/2 H, s); δC 55.9, 25.3, 23.5, 32.0, 47.7, 44.4, 172.3, 178.9, 134.1, 130.1, 128.5, 133.8. Isolation of the antigenic material, X-1, was performed with a reverse-phase HPLC on a Develosil C-30 column (4.6 × 250 mm). The reaction mixture was concentrated and applied to the column equilibrated in a solution of 23% methanol in 0.1% acetic acid. Products were eluted at a flow rate of 0.8 ml/min, the elution being monitored by absorbance at 240 nm. X-1 was isolated (yield, 7 mg), and its chemical structure was characterized by LC-MS and ^{1}H and ^{13}C NMR spectrometries. ^{1}H NMR (CD3OD): δH 1.13 (^{3}H, t, J = 7.60 Hz), 1.32 (2H, m), 1.62–1.93 (4H, m), 2.63 (^{3}H, m), 2.65 (2H, m), 4.00 (2H, dd, J = 6.96, 16.66 Hz), 4.17 (1H, m), 4.35 (2H, m), 7.46 (2H, t, J = 7.68 Hz), 7.56 (1H, t, J = 7.20, 7.48 Hz), 7.62 (1H, d, J = 8.24 Hz), 7.72 (2H, d, J = 8.16 Hz), 8.05 (1H, d, J = 8.20 Hz), 8.38 (1H, s); δC 55.7, 26.0, 23.1, 32.2, 58.7, 44.4, 172.0, 179.4, 134.0, 130.0, 128.3, 133.7.

Protein Carbonyl

An aliquot (0.5 ml) of the protein samples was treated with an equal volume of 0.1% (w/v) 2,4-dinitrophenylhydrazine (DNPH) in 2 N HCl and incubated for 1 h at room temperature. This mixture was treated with 0.5 ml of 20% trichloroacetic acid (w/v, final concentration), and after centrifugation, the precipitate was extracted three times with ethanol/ethyl acetate (1:1, v/v). The protein sample was then dissolved with 2 ml of 8 M guanidine hydrochloride/13 mM EDTA/133 mM Tris solution (pH 7.4), and the UV absorbance was measured at 365 nm. The results were expressed as moles of DNPH incorporated/protein (mol/mol) based on an average absorptivity of 21.0 mM^{-1} cm^{-1} (15).

Amino Acid Analysis

An aliquot (0.1 ml) of the protein samples incubated in the absence or presence of crotonaldehyde was treated with 10 mM EDTA (10 μl), 1 N *NaOH* (10 μl), and 100 mM $NaBH_4$ (10 μl). After incubation for 1 h at 37 °C, the mixture was treated with treated with 10% trichloroacetic acid. After centrifugation at 10,000 × *g* for 3 min, the proteins were hydrolyzed *in vacuo* with 6 N HCl for 24 h at 105 °C. The hydrolysates were then concentrated and dissolved in 50 mM sodium phosphate buffer (pH 7.4). The amino acid analysis was performed using a JEOL JLC-500 amino acid analyzer equipped with a JEOL LC30-DK20 data analyzing system.

In Vitro Peroxidation of LDL

LDL (1.019–1.063 g/ml) was prepared from the plasma of healthy humans by sequential ultracentrifugation and then extensively dialyzed against phosphate-buffered saline (10 mM sodium phosphate buffer, pH 7.2, containing 150 mM NaCl) containing 0.01% EDTA at 4 °C. LDL used for the oxidative modification by Cu^{2+} was dialyzed against a 1000-fold volume of phosphate-buffered saline at 4 °C. The oxidation of LDL was performed by incubating 0.5 mg of LDL with $CuSO_4$ (10 μM) in 1 ml of 50 mM sodium phosphate buffer (pH 7.2) at 37 °C.

Antibody Preparation

Female BALB/c mice were immunized three times with the crotonaldehyde-treated KLH. Spleen cells from the immunized mice were fused with P3/U1 murine myeloma cells and cultured in hypoxanthine/amethopterin/thymidine selection medium. Culture supernatants of the hybridoma were screened using an ELISA, employing pairs of wells of microtiter plates on which were absorbed crotonaldehyde-treated BSA

as the antigen (1 μg of protein/well). After incubation with 100 μl of the hybridoma supernatants, and with intervening washes with Tris-buffered saline, pH 7.8, containing 0.05% Tween 20 (TBS-Tween), the wells were incubated with alkaline phosphatase-conjugated goat anti-mouse IgG, followed by a substrate solution containing 1 mg/ml *p*-nitrophenyl phosphate. Hybridoma cells corresponding to the supernatants that were positive on crotonaldehyde-modified BSA were then cloned by limiting dilution. After repeated screening, four clones were obtained. Among them, clone 82D3 showed the most distinctive recognition of the crotonaldehyde-modified BSA.

Enzyme-linked Immunosorbent Assay

The competitive and non-competitive ELISA were performed as previously described (16).

SDS-Polyacrylamide Gel Electrophoresis

SDS-PAGE was performed according to Laemmli (17). The protein was stained with Coomassie Blue.

Agarose Gel Electrophoresis

Agarose gel electrophoresis of LDL was performed using the TITAN GEL High Resolution Protein System (Helena Laboratories, Saitama, Japan). LDL was stained with Fat Red 7B.

Immunoblot Analysis

A gel was transblotted onto a nitrocellulose membrane, incubated with Block Ace (40 mg/ml) for blocking, washed, and treated with the primary antibody (mAb82D3). This procedure was followed by the addition of horseradish peroxidase conjugated to a goat anti-mouse IgG F(ab')2 fragment and ECL reagents (Amersham Pharmacia Biotech, Buckinghamshire, UK). The bands were visualized by exposure of the membranes to autoradiography film.

Animal Experiments

The ferric nitrilotriacetate (Fe^{3+}-NTA) solution was prepared immediately before use by the method described in a previous study (18) with a slight modification. Briefly, ferric nitrate enneahydrate and the nitrilotriacetic acid disodium salt were each dissolved in deionized water to form 80 and 160 mM solutions, respectively. They were mixed at the volume ratio of 1:2 (molar ratio, 1:4), and the pH was adjusted with sodium hydrogen carbonate to 7.4. Male SPF slc: Wistar rats (Shizuoka Laboratory Animal Center, Shizuoka), weighing 130–150 g (6 weeks of age), were used. They were kept in a stainless steel cage and given commercial rat chow (Funabashi F-2, Chiba) as well as deionized water (Millipore Japan, Osaka) *ad libitum*. Animals received a single intraperitoneal injection of Fe^{3+}-NTA (15 mg Fe/kg of body weight). They were sacrificed at 0, 24, 48 h after the administration. The animals were sacrificed by decapitation. Both kidneys of each animal were immediately removed. One of them was fixed in Bouin's solution, embedded in paraffin, cut at 3-μm thickness, and used for immunohistochemical analyses by an avidin-biotin complex method with alkaline phosphatase (19). Briefly, after deparaffinization with xylene and ethanol, normal rabbit serum (Dako Japan Co., Ltd., Kyoto; diluted to 1:75) for the inhibition of the nonspecific binding of the secondary antibody, a monoclonal antibody (mAb82D3) against crotonaldehyde-modified proteins (0.5 μg/ml), biotin-labeled rabbit anti-mouse IgG serum (Vector Laboratories; diluted 1:300), and avidin-biotin complex (Vector; diluted 1:100) were sequentially used. Procedures using phosphate-buffered saline or the IgG fraction (0.5 μg/ml) of normal mouse serum instead of mAb82D3 antibody against crotonaldehyde-modified proteins showed no or negligible positivity.

RESULTS

Covalent Binding of Crotonaldehyde to Protein

Crotonaldehyde is a strong electrophile, which may readily react with nucleophiles, such as protein. As shown in Fig. 2*A*, binding of the crotonaldehyde to bovine serum albumin was suggested by a slight expanse and mobility shift of the protein bands on the SDS-PAGE analysis. To further evaluate the covalent binding of crotonaldehyde to the protein, we examined the generation of the protein-linked carbonyl groups and changes in the amino acid composition. Spectrophotometric measurement of the protein carbonyls, after their reaction with DNPH, is a simple and accurate technique that has been widely

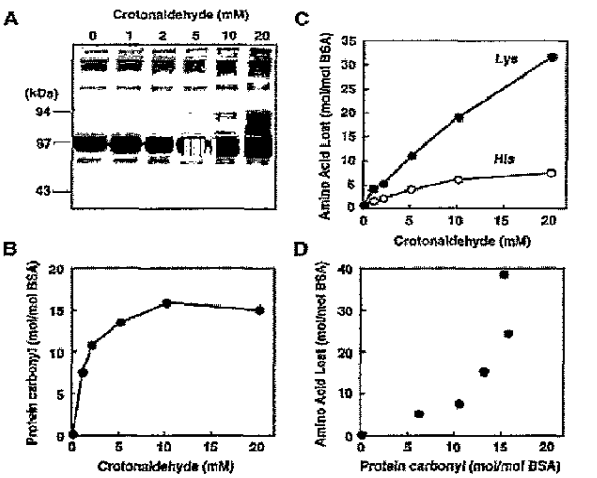

FIG. 2. **Covalent attachment of crotonaldehyde to protein.** BSA (1 mg/ml) was incubated with 0–20 mM crotonaldehyde in 50 mM sodium phosphate buffer (pH 7.4) at 37 °C. *A*, SDS-PAGE analysis; *B*, introduction of carbonyl groups into protein upon reaction with crotonaldehyde. The protein carbonyl content was determined by the procedure using DNPH. *C*, loss of histidine (○) and lysine residues (●). An aliquot (0.1 ml) was taken from the reaction mixture and the amount of amino acids was determined by amino acid analysis as described in the "Experimental Procedures." *D*, relationship between protein carbonyls and loss of amino acids.

used to reveal increased levels of covalently modified proteins during aging and disease (1–3). As shown in Fig. 2*B*, exposure of BSA to crotonaldehyde resulted in a dose-dependent increase in the protein carbonyl formation. The incorporation of crotonaldehyde into the protein was accompanied by selective loss of histidine and lysine residues (Fig. 2*C*). However, as shown in Fig. 2*D*, the stoichiometry between the loss of amino acids and the increase in protein carbonyls did not show a linear correlation. At low concentrations of crotonaldehyde (≤2.5 mM), the sum of the amounts of lysine and histidine residues lost was almost equal to the amount of protein carbonyl groups detected; whereas, even after the protein carbonyl content leveled off, the loss of amino acids still continued when the concentration of crotonaldehyde was raised from 10 to 20 mM. These data suggest that crotonaldehyde at low concentrations mainly forms carbonyl adducts, whereas, at high concentrations, it preferentially forms non-carbonyl adducts, in addition to carbonyl adducts, in the protein.

Identification of Crotonaldehyde Adducts Possessing a Carbonyl Function

To characterize the crotonaldehyde adducts possessing a carbonyl function, the histidine and lysine derivatives were incubated with crotonaldehyde, and the products were characterized by LC-MS and NMR spectroscopy (^1H and ^{13}C NMR).

Crotonaldehyde-Histidine Adduct—As shown in Fig. 3*A*, the incubation of N^{α}-acetylhistidine with crotonaldehyde generated a single product. The LC-MS analysis of the product showed a pseudomolecular ion peak at *m/z* 268 $(M+H)^+$, suggesting that it was composed of one molecule of N^{α}-acetylhistidine and one molecule of crotonaldehyde. Support for modification of the imidazole nitrogens was shifts downfield of the imidazole vinyls (δH 7.59 and 9.07; δC 117.76 and 134.1) in the ^1H NMR spectrum. The presence of the β-substituted butanal moiety was clearly observed: δH 1.46 (-C*H*3), 3.10 (-C*H*2-), 4.95 (>C*H*-), and 9.58 (-C*H*O); δC 20.78 (-C*H*3), 48.38 (-C*H*2-), 50.39 (>C*H*-), and 200.13 (-C*H*O). This was also confirmed by the

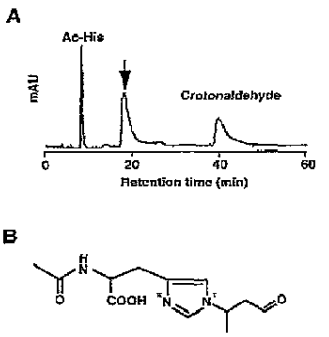

FIG. 3. **Reaction of N^{α}-acetylhistidine with crotonaldehyde.** The reaction mixture containing 100 mM N^{α}-acetylhistidine and 100 mM crotonaldehyde in 50 mM sodium phosphate buffer (pH 7.2) was incubated for 48 h at 37 °C. *A*, HPLC profile of the reaction mixture. The reaction mixture was analyzed by a reverse-phase HPLC using a Develosil ODS-HG-5 column (4.6 × 250 mm) equilibrated in 0.1% trifluoroacetic acid at a flow rate of 0.8 ml/min. The elution profiles were monitored by absorbance at 200–400 nm. A major product is indicated by the *arrow*. *B*, chemical structure of the β-substituted N^{τ}-butanal derivative of N^{α}-acetylhistidine.

^{1}H-detected multiple-bond heteronuclear multiple quantum coherence spectrum (HMBC) experiments (data not shown). Thus, the structure of the product was determined to be the β-substituted butanal derivative of N^{α}-acetylhistidine (Fig. 3*B*). It is suggested that the adduct is generated from the nucleophilic attack of the imidazole nitrogen on the ethylenic bond of crotonaldehyde (Michael addition). Therefore, the adduct, we first speculated, was a mixture of the isomeric form of the N^{π}- and N^{τ}-substituted adducts of the imidazole ring. However, the NMR spectra apparently indicated that the reaction was exclusively occurring at one position. Our assignment of the structure involving the N^{τ} alkylation was on the basis that the methine proton of the butanal moiety was correlated with the two imidazole vinyls (C-2 and C-5) in the HMBC spectrum (data not shown). Our observation of exclusive N^{τ} alkylation is not without precedent (20) and must reflect a combination of the high chemoselectivity and large steric requirements of this particular Michael addition reaction, as opposed to, for example, simple alkylation by primary alkyl halides.

Crotonaldehyde-Lysine Adduct—Upon incubation of the lysine derivative (N^{α}-hippuryllysine) with crotonaldehyde, two major products (P-1 and P-2) were detected (Fig. 4*A*). P-1 was suggested to be the butanal derivative of N^{α}-hippuryllysine by LC-MS (m/z 378 [M + H$^+$]) (Fig. 4*B*), while we were unable to isolate the adduct. P-2 was isolated and submitted for structural characterization. The LC-MS analysis of the product showed a pseudomolecular ion peak at m/z 430 (M+H)$^+$, suggesting that it was composed of one molecule of N^{α}-hippuryllysine and two molecules of crotonaldehyde. In analogy with the acrolein reaction (21), the ^{1}H and ^{13}C NMR spectra of the product suggested the presence of a 3-formyl-3,4-dehydropiperidino (FDP) moiety. In addition, the adduct appeared to have two methyl groups: δH 1.19 (^{3}H, m) and 1.29 (^{3}H, d, J = 6.76 Hz); δC 16.2 and 18.0. An HMBC experiment showed the correlations of methyl protons (1.29 ppm) to C-2 and C-3 and another methyl proton (1.19 ppm) to C-5 and C-6. Taken together, P-2 was determined to be the N^{α}-hippuryl derivative of N^{ϵ}-(2,5-dimethyl-3-formyl-3,4-dehydropiperidino)lysine (dimethyl-FDP-lysine) (Fig. 4*B*). The findings that both acrolein and crotonaldehyde generate the FDP-lysine adducts suggest that this type of condensation reaction is characteristic of the reaction for 2-alkenals with primary amines. Indeed, upon

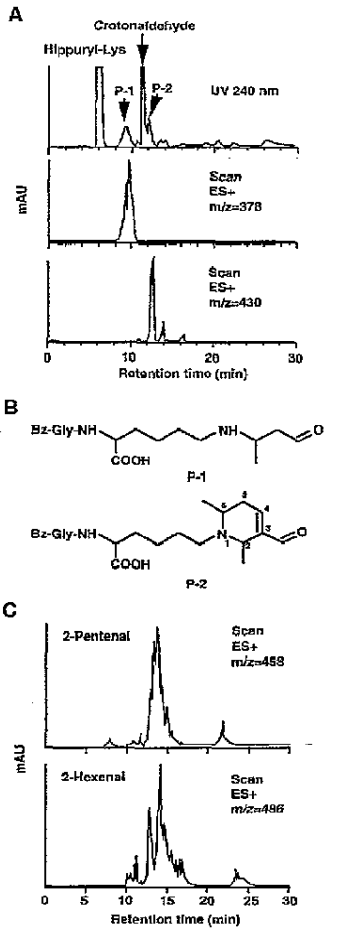

FIG. 4. **Reaction of N^{α}-hippuryllysine with crotonaldehyde.** The reaction mixture containing 100 mM N^{α}-hippuryllysine and 100 mM crotonaldehyde in 50 mM sodium phosphate buffer (pH 7.2) was incubated for 24 h at 37 °C. *A*, LC-MS analysis of crotonaldehyde-lysine adducts. *Top*, HPLC profile of the reaction mixture. The reaction mixture was analyzed by a reverse-phase HPLC using a Develosil ODS-MG-5 column (4.6 × 250 mm) equilibrated in a solution of 20% methanol in 0.1% acetic acid at a flow rate of 0.8 ml/min. The elution profile was monitored by absorbance at 240 nm. *Middle* and *bottom*, selected ion current chromatograms obtained from LC-MS analysis monitored with m/z 378 and m/z 430. *B*, chemical structures of the N^{α}-hippuryl derivatives of butanallysine and dimethyl-FDP-lysine. *C*, selected ion current chromatograms obtained from LC-MS analysis for FDP-type adducts upon incubation of N^{α}-hippuryllysine with 2-pentenal (*upper*) and 2-hexenal (*lower*). The 2-pentenal-derived FDP adducts and 2-hexenal-derived FDP adducts were monitored with m/z 458 and 486, respectively.

reaction with N^{α}-hippuryllysine, the 2-alkenals, such as 2-pentenal and 2-hexenal, generated products that were suggested to be diethyl-FDP-lysine and dipropyl-FDP-lysine, respectively, by the LC-MS analysis (Fig. 4*C*).

Thus, upon reaction with the histidine and lysine derivatives, crotonaldehyde predominantly generated the butanal and FDP adducts. Notably, they all have free aldehyde groups. To examine whether these adducts indeed possess a carbonyl function, we exposed them to excess DNPH, and the products were analyzed by a reverse-phase HPLC. As shown in Fig. 5, they indeed reacted with the carbonyl reagent and provided the new products. The LC-MS analysis of the products gave pseudomolecular ion peaks (M+H)$^+$ at m/z 446 and 608, which

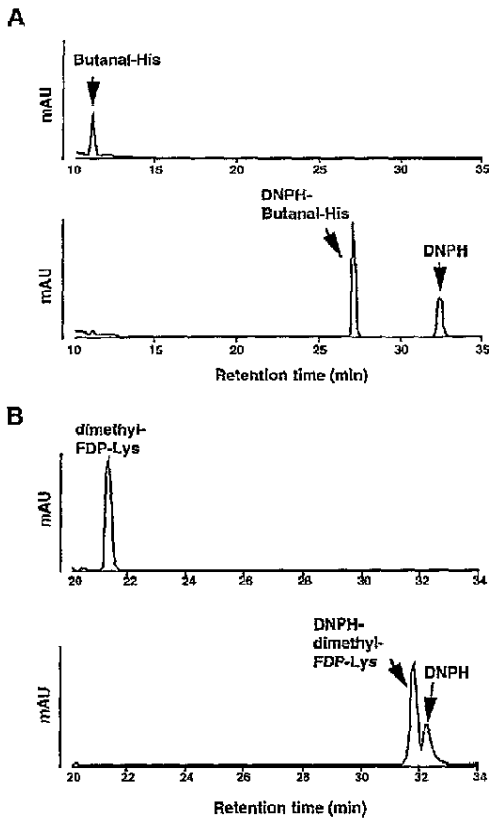

FIG. 5. **DNPH derivatization of crotonaldehyde adducts.** *A*, HPLC profiles of DNPH-treated (*lower*) and untreated (*upper*) N^{α}-acetyl-N^{ϵ}-butanalhistidine. *B*, HPLC profiles of DNPH-treated (*lower*) and untreated (*upper*) N^{α}-hippuryl-dimethyl-FDP-lysine. An aliquot of the crotonaldehyde adducts was treated with an equal volume of 0.1% (w/v) DNPH in 2 N HCl and incubated for 1 h at room temperature. The DNPH-treated and untreated samples were analyzed with a reverse-phase HPLC using a Develosil ODS-MG-5 column (4.6 × 250 mm). The products were eluted with a linear gradient of 0.1% trifluoroacetic acid in water (solvent A)-acetonitrile (solvent B) (time = 0, 100% A; 60 min, 0% A), at a flow rate of 0.8 ml/min. The elution profiles were monitored by absorbance at 195–650 nm.

corresponded to the expected dinitrophenylhydrazone derivatives of the butanalhistidine and dimethyl-FDP-lysine adducts, respectively. The formation of these adducts may therefore contribute to the generation of carbonyl groups in the protein exposed to crotonaldehyde.

Monoclonal Antibody Directed to the Protein-bound Crotonaldehyde

There is increasing evidence that aldehydes endogenously generated during the degradation process of biological molecules are involved in many of the pathophysiologies (5). Major sources of reactive aldehydes *in vivo* have been suggested to be lipid peroxidation, glycation, and amino acid oxidation (6). Crotonaldehyde has been reported to be produced during lipid peroxidation (11, 12); however, as far as we know, very few papers have addressed the endogenous production of the crotonaldehyde protein adduct *in vivo*. Accordingly, to evaluate whether the adduct is produced *in vivo*, we attempted to raise the monoclonal antibody specific to the protein-bound crotonaldehyde. Mice were immunized with the crotonaldehyde-modified KLH and, during the preparation of the monoclonal antibodies, hybridomas were selected by the reactivities of the culture supernatant to the crotonaldehyde-modified BSA. Among the six clones obtained, the clone 82D3 showed the most distinctive recognition of the crotonaldehyde-modified BSA.

Isolation of the Antigenic Crotonaldehyde-Lysine Adduct

Characterization of the antibodies' ability to recognize specific molecular targets in their native three-dimensional conformation is critical to the use of these reagents. Therefore, we attempted to identify the structure of the epitope recognized by mAb82D3. As shown in Fig. 6*A*, the monoclonal antibody showed a strong immunoreactivity not only with crotonaldehyde but also with the crotonaldehyde analogs, such as 2-pentenal and 2-hexenal. Binding of the crotonaldehyde-modified protein to mAb82D3 was scarcely inhibited by the reaction mixtures of crotonaldehyde/cysteine and crotonaldehyde/histidine but significantly inhibited by the reaction mixture of crotonaldehyde/lysine (Fig. 6*B*), suggesting that mAb82D3 recognizes a lysine adduct as the epitope. To identify the crotonaldehyde-lysine adduct recognized by mAb82D3, the immunoreactivity with the reaction products of crotonaldehyde with N^{α}-hippuryllysine was characterized. As shown in Fig. 6*C*, the ELISA analysis of the HPLC fractions for immunoreactivity with mAb82D3 showed that the antibody had immunoreactivity with multiple fractions, including the fraction containing dimethyl-FDP-lysine and fractions 1 and 2. The ratio of immunoreactivities to the yields of each fraction indicated that the antibody predominantly reacted with fractions 1 and 2. Both fraction 1 and the dimethyl-FDP adduct did not lose antigenicity even after acid hydrolysis, suggesting the good stability of the epitope structures (Fig. 6*D*). Fraction 2 was found to be a mixture of multiple products, and no attempt was made to isolate an antigenic adduct from this fraction. Although, a reverse-phase HPLC analysis of fraction 1 was demonstrated to contain one major product (X-1) (Fig. 6*E*). As shown in Fig. 6*F*, X-1 was found to be a potent antigenic crotonaldehyde-lysine adduct recognized by mAb82D3.

Identification of the Antigenic Crotonaldehyde-Lysine Adduct

The structure of X-1 was characterized by LC-MS, UV, and ^{1}H and ^{13}C NMR. Compared with the ^{13}C NMR spectra between N^{α}-hippuryllysine and the product, eight signals (δC 14.8, 20.0, 26.0, 130.7, 143.8, 144.5, 145.9, and 153.3) remained in the ^{13}C NMR spectrum of the product, which seemed to originate from two molecules of crotonaldehyde in the reaction with N^{ϵ}-amine of N^{α}-hippuryllysine. The five signals (δC 130.7, 143.8, 144.5, 145.9, and 153.3) suggested the presence of an aromatic ring. The remaining three signals corresponded to two methyls (δH 1.13/δC 14.8; δH 2.63/δC 20.0) and one methylene (δH 2.65/δC 26.0). In addition, the UV spectrum of X-1 exhibited a $\lambda_{max}(\epsilon)$ of 240 (*N*-benzoyl) and 276 nm. These data suggested that the product was composed of one pyridinium ring and one ethyl group and one methyl group. This assumption was supported by the LC-MS analysis of the product showing the $(M+H)^{+}$ peak at *m/z* 412. An HMBC experiment showed the correlations of the ε-CH2 protons and methyl protons (δH 2.63) to δC 153.3 (C-2) but a correlation of the ethyl protons to C-2 was not observed, indicating the presence of the methyl group at C-2 position (Fig. 7). In addition, the HMBC experiment also showed the correlations of the ε-CH2 protons to C-6, H-6 to *C*H2 (δC 26.0), C-2, and C-4 (1.29 ppm), *CH*3 (δH 1.13) to *C*H2 (δC 26.0) and C-5. This was in agreement with the proposed structure (Fig. 7). Based on these characteristics, it was determined that the product was a novel crotonaldehyde-lysine adduct, N^{α}-hippuryl-N^{ϵ}-(5-ethyl-2-methylpyridinium)-lysine (EMP-lysine).

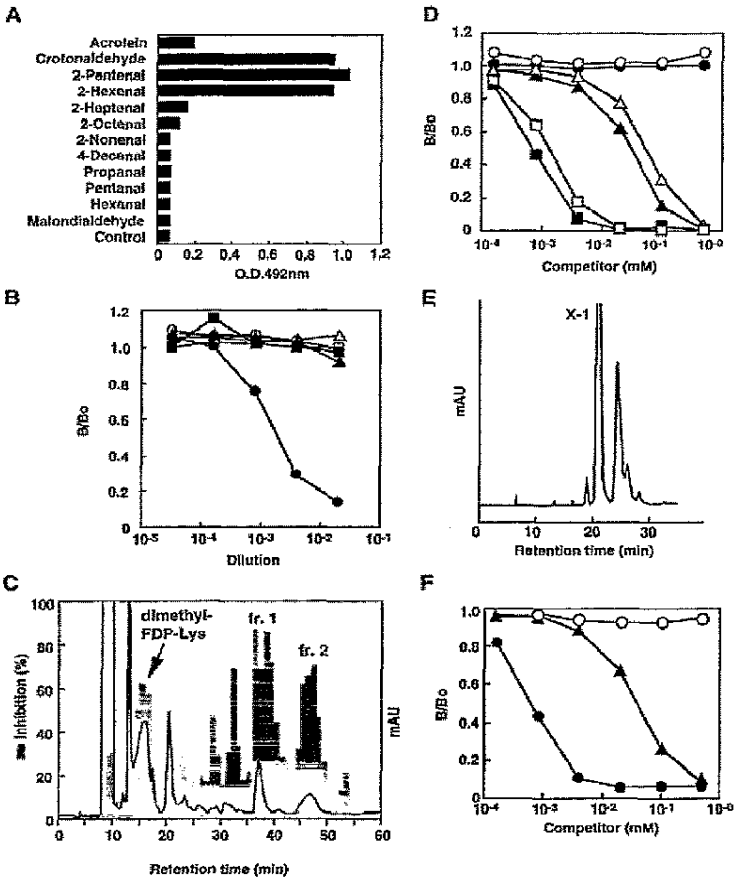

FIG. 6. **Specificity of mAb82D3.** *A*, immunoreactivity of mAb82D3 to the aldehyde-treated protein. Affinity of mAb82D3 was determined by a direct ELISA using aldehyde-treated BSA as the absorbed antigen. A coating antigen was prepared by incubating 1 mg of BSA with 10 mM aldehyde in 1 ml of 50 mM sodium phosphate buffer, pH 7.4, for 2 h at 37 °C. *B*, competitive ELISA analysis with the reaction mixtures of amino acid derivatives and crotonaldehyde. Competitors were prepared by incubating 100 mM amino acid derivatives, N^{α}-acetylcysteine, N^{α}-acetylhistidine, or N^{α}-hippuryllysine, in the presence or absence of crotonaldehyde (100 mM), in 50 mM sodium phosphate buffer (pH 7.2) for 24 h at 37 °C. Competitors: □, N^{α}-acetyllysine; △, N^{α}-acetylhistidine; ○, N^{α}-hippuryllysine; ■, crotonaldehyde/N^{α}-acetylcysteine; ▲, crotonaldehyde/N^{α}-acetylhistidine; ●, crotonaldehyde/N^{α}-hippuryllysine. *C*, competitive ELISA analysis of HPLC fractions for immunoreactivity with mAb82D3. The reaction was performed by incubating 100 mM N^{α}-hippuryllysine with 10 mM crotonaldehyde in 10 ml of 0.1 M sodium phosphate buffer (pH 7.4) at 37 °C for 24 h. *Solid line*, profile of UV absorbance at 240 nm. *Bar*, competitive ELISA analysis. *D*, competitive ELISA analysis with N^{α}-hippuryllysine, N^{α}-hippuryl-dimethyl-FDP-lysine, fraction 1, and their hydrolysates. The acid hydrolysis was carried out *in vacuo* with 6 N HCl for 24 h at 105 °C. Competitors: ●, N^{α}-hippuryllysine; ○, N^{α}-hippuryllysine (hydrolysis); ▲, N^{α}-hippuryl-dimethyl-FDP-lysine; △, N^{α}-hippuryl-dimethyl-FDP-lysine (hydrolysis); ■, fraction 1; □, fraction 1(hydrolysis). *E*, HPLC analysis of fraction 1. Conditions: column, Develosil C-30 column (4.6 × 250 mm); mobile, 23% methanol in 0.1% acetic acid; flow rate, 0.8 ml/min; absorbance, 240 nm. *F*, competitive ELISA analysis with N^{α}-hippuryllysine, N^{α}-hippuryl-dimethyl-FDP-lysine, and X-1. Competitors: ○, N^{α}-hippuryllysine; ▲, N^{α}-hippuryl-dimethyl-FDP-lysine; ●, X-1.

Formation of EMP-Lysine in Crotonaldehyde-modified Protein

To assess the formation of EMP-lysine in proteins, we first sought to detect the adduct in the hydrolyzed samples of authentic N^{α}-hippuryl-EMP-lysine. Upon acid hydrolysis followed by amino acid analysis of N^{α}-hippuryl-EMP-lysine, glycine and a new peak (Fig. 8*A*, indicated by the *arrow*), presumably EMP-lysine, which was distinguishable from the other amino acids, was detected (Fig. 8*A*, *lower*). In addition, the same peak was detected in the hydrolysate of BSA treated with crotonaldehyde (Fig. 8*A*, *upper*). Incubation of the protein with crotonaldehyde resulted in the dose-dependent formation of the putative EMP-lysine adduct (Fig. 8*B*), which was accompanied by a dramatic increase in the immunoreactivity with mAb82D3 (Fig. 8*C*).

Formation of Immunoreactive Materials with mAb82D3 in the Renal Proximal Tubules of Rats Exposed to Fe^{3+}-NTA

The production of immunoreactive materials with mAb82D3 *in vivo* was assessed in a rat renal carcinogenesis model with Fe^{3+}-NTA. It has been shown that iron overload using Fe^{3+}-NTA induces acute renal proximal tubular necrosis, a consequence of oxidative tissue damage, that eventually leads to a high incidence of renal adenocarcinoma in rodents (22, 23). The location of the positive cells with mAb82D3 was assessed by an immunohistochemical study. The kidneys were excised at the time of sacrifice and then fixed with Bouin's fixative. The hematoxylin and eosin-stained sections of the paraffin-embedded tissues were analyzed for histological damage. The morphological changes in the kidneys of rats treated with Fe^{3+}-NTA *versus* time are very similar to previous reports on ddY

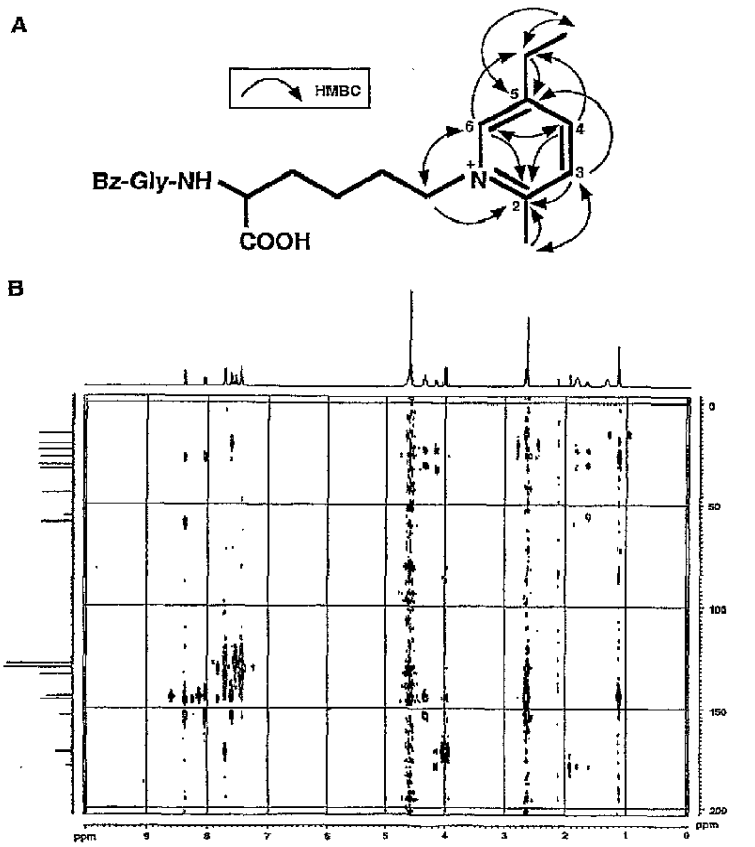

FIG. 7. **H^1-detected multiple-bond heteronuclear multiple quantum coherence (HMBC) spectrum of X-1.** The proposed structure (*A*) and the HMBC spectrum (*B*) of X-1. *Bz*, benzoyl group. The spectrum was acquired in D_2O. The connectivities observed in the pyridinium ring moiety are indicated by *arrows* in *Panel A*.

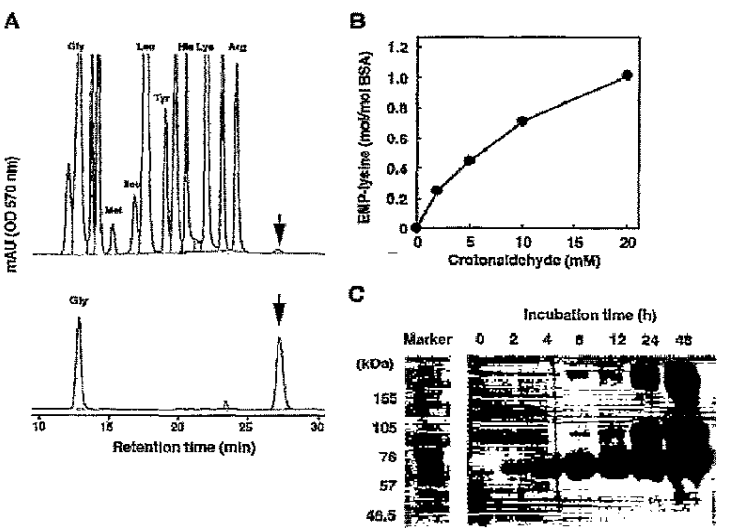

FIG. 8. **Formation of EMP-lysine in the crotonaldehyde-modified BSA.** BSA (1.0 mg/ml) was incubated with 1 mM crotonaldehyde in 50 mM sodium phosphate buffer (pH 7.4) at 37 °C. Loss of lysine and the formation of EMP-lysine were determined by amino acid analysis as already described. *A*, detection of EMP-lysine by amino acid analysis. *Lower*, hydrolysate of authentic N^{α}-hippuryl-EMP-lysine; *upper*, hydrolysate of crotonaldehyde-modified BSA. *B*, dose-dependent formation of putative EMP-lysine adduct in the crotonaldehyde-modified BSA. EMP-lysine generated in the protein was quantitated by a calibration curve obtained from the acid hydrolysis followed by amino acid analysis of authentic N^{α}-hippuryl-EMP-lysine (0–0.4 mM). *C*, immunoblot analysis of crotonaldehyde-modified BSA with mAb82D3.

mice (18, 24). In the control rat kidney, an almost negligible level of immunoreactivity was observed (Fig. 9*A*). The immunoreactivities were found in some of the the renal proximal tubular cells 24 h after the administration of 15 mg of Fe/kg of body weight of Fe^{3+}-NTA (Fig. 9*B*). Intense immunoreactivities were also observed at 48 h in the degenerating cells, which were indicated by pyknosis (Fig. 9*C*). Some of the proteinaceous casts were also stained. Significantly, immunoreactivities were found not only in the cytoplasm but in some of the nuclei. This pattern of distribution in the rat kidney is consistent with that of the distribution of membrane lipid peroxidation products and their conjugates with cytosolic proteins (25), suggesting a

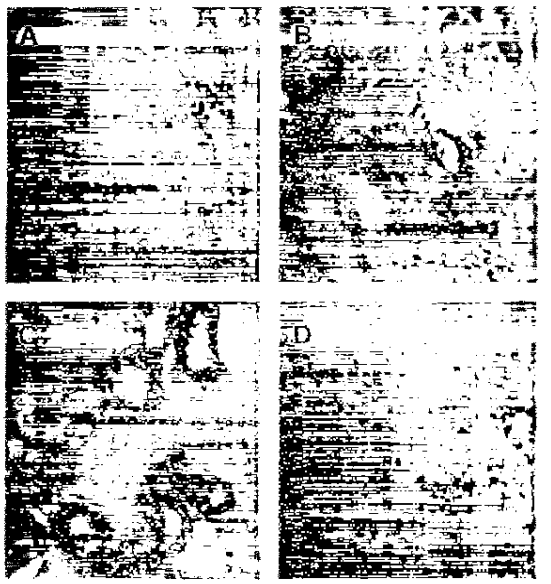

FIG. 9. **Immunohistochemistry of renal cortex with mAb82D3 (× 400).** *A*, untreated control. *B*, 24 h after Fe^{3+}-NTA injection. *C*, 48 h after Fe^{3+}-NTA injection. *D*, for a competitive experiment, mAb82D3 preincubated with an excess of N^{α}-hippuryl-EMP-lysine was used.

correlation between the production of the crotonaldehyde/2-alkenals and oxidative stress. Pre-absorption of the antibody with EMP-lysine completely abolished the immunostaining (Fig. 9*D*), indicating the specific reactivity of the antibody with the epitope.

Lipid Peroxidation Is an Endogenous Pathway for the Formation of Crotonaldehyde/2-Alkenals and Its Protein Adducts

The most likely endogenous source of crotonaldehyde/2-alkenals is polyunsaturated fatty acids (11, 12). To test whether immunoreactive materials with mAb82D3 are produced during lipid peroxidation, we first analyzed the production of immunoreactive materials in the Cu^{2+}-oxidized LDL. Incubation of LDL with Cu^{2+} led to the oxidation of the LDL as assessed by the formation of thiobarbituric acid reactive substances (data not shown). After separation by agarose gel electrophoresis, the native form of the LDL appeared as a single protein band that was readily visualized by Fat Red 7B staining (Fig. 10*A*); however, the LDL incubated with 5 μM Cu^{2+} exhibited enhanced anodic mobility compared with the native LDL, indicating the increased negative charge of the molecule probably due to the modification of the ϵ-amino group in the lysine residues. An agarose gel electrophoresis/immunoblot analysis of the Cu^{2+}-oxidized LDL using mAb82D3 revealed the formation of immunoreactive materials, which were not detected in the native LDL. Involvement of lipid peroxidation was further attested by an alternative experiment, in which polyunsaturated fatty acids were incubated with an iron/ascorbate-mediated free radical generating system in the presence of protein. As shown in Fig. 10*B*, the iron/ascorbate-mediated oxidation of α-linolenic acid in the presence of BSA resulted in a time-dependent increase in the antigenicity of the protein, whereas the incubation with either iron or ascorbate alone scarcely generated any antigenic materials (data not shown). Interestingly, BSA treated with the iron/ascorbate/α-linolenic acid system revealed a >200-kDa protein that exhibited a strong immunoreactivity with mAb82D3. These data

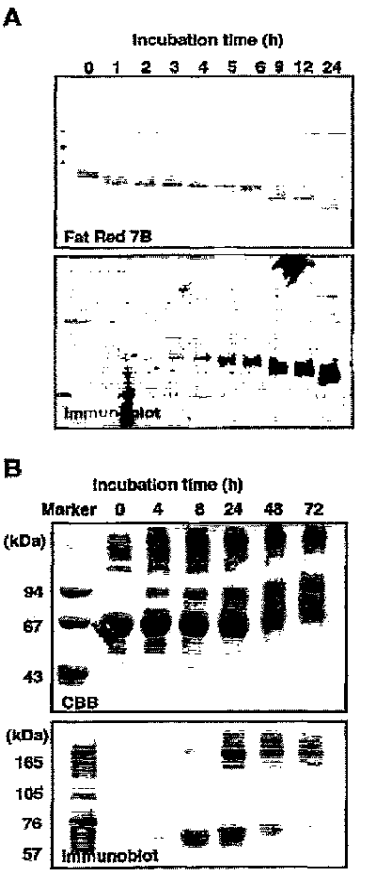

FIG. 10. ***In vitro* formation of immunoreactive materials *via* lipid peroxidation.** *A*, LDL (0.5 mg) was incubated with 5 μM Cu^{2+} in 1 ml of 50 mM sodium phosphate buffer (pH 7.2) at 37 °C. *Upper*, agarose gel electrophoresis; *lower*, agarose gel electrophoresis/immunoblot analysis with mAb82D3. *B*, iron-catalyzed oxidation of α-linolenic acid in the presence of BSA was performed by incubating BSA (1 mg/ml) with 2 mM α-linolenic acid in the presence of 10 μM Fe^{3+} and 1 mM ascorbate in 0.1 ml of 50 mM sodium phosphate buffer (pH 7.4) at 37 °C. *Upper*, SDS-PAGE; *lower*, immunoblot analysis with mAb82D3.

strongly suggest that lipid peroxidation is essential for the endogenous production of crotonaldehyde/2-alkenals *in vivo*.

DISCUSSION

A growing body of evidence suggests that many of the effects of cellular dysfunction under oxidative stress are mediated by products of non-enzymatic reactions, such as the peroxidative degradation of polyunsaturated fatty acids. Lipid peroxidation proceeds by a free radical chain reaction mechanism and yields lipid hydroperoxides as major initial reaction products. Subsequently, the decomposition of lipid hydroperoxides generates a number of breakdown products that display a wide variety of damaging actions. A number of reactive aldehydes derived from lipid peroxidation have been implicated as causative agents in cytotoxic processes initiated by the exposure of biological systems to oxidizing agents (5). *In vitro* studies of the detection of protein-bound crotonaldehyde during the peroxidation of LDL (Fig. 10*A*) and the metal-catalyzed oxidation of α-linolenic acid in the presence of protein (Fig. 10*B*) demonstrated that substantial amounts of crotonaldehyde/2-alkenals might be generated during the peroxidation of polyunsaturated

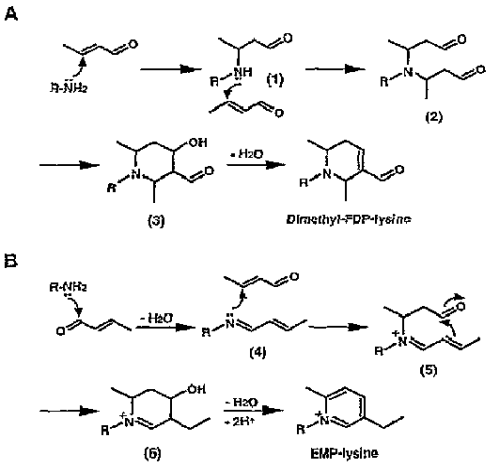

SCHEME 1. **Proposed mechanisms for the formation of dimethyl-FDP-lysine (*A*) and EMP-lysine (*B*).**

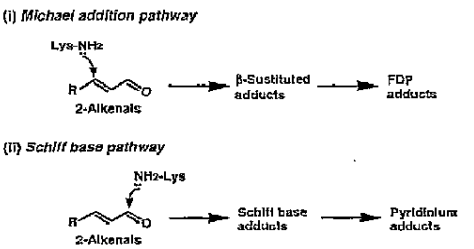

SCHEME 2. **Lysine adduction with 2-alkenals.** The 2-alkenals undergo nucleophilic addition of the lysine amino group at the C-3 double bond and the C-1 aldehyde moiety to form Michael adducts, including β-substituted and FDP adducts (*Michael addition pathway*), and pyridinium adducts *via* Schiff base adducts (*Schiff base pathway*), respectively.

fatty acids. We have observed that LDL peroxidation produces multiple products that react with DNPH, as monitored by reverse-phase HPLC, and one of the major products comigrates with the DNPH derivative of authentic crotonaldehyde.[2] In addition, the same product has also been detected in the autoxidation of polyunsaturated fatty acids with an iron/ascorbate-mediated free radical generating system.[2] These data strongly suggest that the peroxidation of polyunsaturated fatty acids under oxidative stress represents a potential endogenous pathway for the production of crotonaldehyde *in vivo*. It should also be noted that, among polyunsaturated fatty acids, crotonaldehyde was most efficiently produced from linoleate and α-linolenic acid; whereas, others, including arachidonate, *cis*-5,8,11,14,17-eicosapentaenoic acid, and *cis*-4,7,10,13,16,19-docosahexaenoic acid, scarcely produced crotonaldehyde.[2] This is a striking contrast to the previous observation that arachidonate and these ω3-polyunsaturated fatty acids represent excellent sources of acrolein (21). Although the mechanism of the formation of crotonaldehyde during lipid peroxidation has not yet been experimentally resolved, there may be no doubt that crotonaldehyde is a physiologically important aldehyde that could be ubiquitously generated under oxidative stress. In addition, because crotonaldehyde is one of the most reactive and cytotoxic aldehydes (5), it could be a major causal factor that contributes to the development of tissue damage under oxidative stress.

Protein carbonyls represent a putative marker of oxidatively modified proteins and can be conveniently measured by sensitive methods, particularly those using DNPH, which reacts with carbonyl groups to generate dinitrophenylhydrazones with characteristic absorbance maxima at 360–390 nm (15). It has been established that protein carbonyls accumulate on tissue proteins during aging (26) and disease development. Increased levels of protein carbonyls are associated with Alzheimer's disease (27), progeria and Werner's syndrome (28), amyotrophic lateral sclerosis (29), and respiratory distress syndrome (30), among others. Although the experimental evidence is so far mostly correlative, it lends strong support to the hypothesis that the protein carbonyl content of tissues reflects the fraction of oxidatively damaged protein with impaired function and might, therefore, be at the root of disease- and aging-related functional losses (31). It has been shown that, in addition to the oxidatively modified proteins, carbonyl-containing adducts can be generated through the reaction of proteins with sugars (glycation) and lipid peroxidation products, such as 4-hydroxy-2-nonenal and malondialdehyde (32, 33). We found in this study that the exposure of proteins to crotonaldehyde dramatically generated protein carbonyls (Fig. 2). In addition, upon incubation with amino acid derivatives, crotonaldehyde generated the butanal and FDP adducts, which possess a carbonyl function (Figs. 3–5). These adducts may represent carbonyl derivatives generated in the oxidatively modified protein *in vivo*. In addition to the large body of data demonstrating the formation of carbonyl groups by metal-catalyzed oxidation systems, our present findings add crotonaldehyde to a growing list of reactive species that can introduce carbonyl groups into proteins.

The susceptibility of 2-alkenals to nucleophilic addition first prompted us to characterize a thioether adduct via a Michael addition mechanism. Thiols are particularly strong nucleophiles, and α,β-unsaturated ketones are, indeed, known to enzymatically or nonenzymatically react with thiols such as glutathione and cysteine to give the thiol conjugates (5). LC-MS monitoring indeed revealed that crotonaldehyde readily reacted with *N*-acetylcysteine, giving only a Michael addition adduct presumably as a mixture of epimers at the C-3 position.[2] Likewise, in the previous observation (34), however, we were unable to isolate the adduct. Isolation of the crotonaldehyde-lysine Michael adduct was not feasible either, although its formation was verified by the detection with LC-MS (Fig. 4*A*). In either case, the adductions may be readily reversed in aqueous buffer. This may lead to the reversible binding of crotonaldehyde to the cysteine and lysine residues of the proteins. In contrast, the crotonaldehyde-histidine Michael adduct is readily isolated and is stabilized toward the retro-Michael addition reaction (Fig. 3), apparently due to the poorer leaving group ability of the imidazole over the sulfhydryl and primary amine at neutral pH.

In this study, we isolated and identified a stable adduct (dimethyl-FDP-lysine), resulting from the Michael addition reaction of crotonaldehyde with the ε-amino group of lysine. The likely origin of the adducts is outlined in Scheme 1*A*; crotonaldehyde undergoes nucleophilic addition of the lysine amino group at the double bond (C-3) to form a secondary amine derivative (1), which further reacts with another crotonaldehyde molecule via a Michael addition to generate an imine derivative (2 and 3). Aldol condensation followed by dehydration reactions lead to the formation of dimethyl-FDP-lysine. The formation of the FDP-type adduct was first reported in the lysine modification with acrolein (21). In addition, the FDP adducts were also detected in the reaction of other 2-alkenals, such as 2-pentenal and 2-hexenal, with the lysine derivative

[2] K. Ichihashi and K. Uchida, unpublished observations.

(Fig. 6). Therefore, it is hypothesized that the condensation reaction *via* formation of the Michael addition-derived imine derivatives is characteristic of the reaction of 2-alkenals with primary amines ("Michael addition pathway") (Scheme 2). It is of interest that a large excess of aldehyde over the amine was not necessarily needed to ensure the formation of the FDP adducts. The use of equimolar quantities afforded adducts mainly containing two molecules of crotonaldehyde per lysine molecule. Although this suggested at the time that crotonaldehyde was inherently biased toward condensation (*e.g.* aldol) chemistry, our ability to obtain FDP adducts from equimolar crotonaldehyde-lysine reactions indicates that the amine is responsible for stimulating the aldehyde condensations, presumably *via* formation of Michael adducts. On the other hand, lysine adduction with 2-alkenals generates another class of condensation adducts *via* Schiff base formation ("Schiff base pathway") (Scheme 2). Upon investigation of an antigenic adduct recognized by the antibody (mAb82D3), we unexpectedly identified the Schiff base-derived pyridinium adduct (EMP-lysine). The formation of EMP-lysine can be reasonably explained by the mechanism involving the formation of a Schiff base derivative (**4**) (Scheme 1*B*). The Schiff base further reacts with a second crotonaldehyde molecule via a Michael addition to generate an imine derivative (**5** and **6**). This intermediate then undergoes an intermolecular aldol condensation followed by dehydration to form the EMP-lysine. This adduct was detected as a minor product in the reaction of crotonaldehyde with the lysine derivative. However, formation of the pyridinium adducts has been reported to be a dominant pathway for modification of the primary amine with 2-alkenals, such as 2-hexenal and 2-octenal (35–37). It has been suggested that the Schiff bases derived from these 2-alkenals acts as an electrophile and the enolate anion of the second aldehyde moiety is required as a nucleophile when attacking the Schiff base. Whereas, EMP-lysine is likely formed through a different mechanism involving the nucleophilic (Michael) addition of the nitrogen from the dienamine tautomer of the initial Schiff base on C-3 of the second crotonaldehyde (Scheme 1*B*). The formation of the lysine-pyridinium species in proteins may result in the placement of a fixed, positive charge on the ε-amino group.

Immunologic detection is a powerful tool that can be used to evaluate the presence of a desired target and its subcellular localization. Major advantages of this technique over biochemical approaches are the evaluation of small numbers of cells or archival tissues that may otherwise not be subject to analysis. In this study, we obtained a murine monoclonal antibody, mAb82D3, that clearly distinguished the crotonaldehyde-modified protein from the native protein. This antibody appeared to be highly specific for the protein-bound 2-alkenals, including crotonaldehyde, 2-pentenal, and 2-hexenal. In addition, we identified the Schiff base-derived EMP-lysine as the major epitope of mAb82D3. The presence of immunoreactive materials with mAb82D3 *in vivo* was demonstrated in the kidney of rats exposed to Fe^{3+}-NTA. The iron chelate was originally used for an experimental model of iron overload (38). Later, repeated intraperitoneal injections of Fe^{3+}-NTA were reported to induce acute and subacute renal proximal tubular necrosis and a subsequent high incidence (60–92%) of renal adenocarcinoma in male rats and mice (22, 23). A single injection of Fe^{3+}-NTA causes a number of time-dependent morphological alterations in the structure and the function of the renal proximal tubular cells and their mitochondria. During the early stage of injury, typical cellular changes are the loss of brush border, cytoplasmic vesicles, mitochondrial disorganization, and dense cytoplasmic deposits in the proximal tubular cells. Most of the damaged epithelia shows the typical appearance of necrotic cells, and more than half of the proximal tubular cells are removed. It has been suggested that oxidative stress is one of the basic mechanisms of Fe^{3+}-NTA-induced acute renal injury and is closely associated with renal carcinogenesis (39). The present *in vivo* study has shown that the carcinogenic aldehydes, such as crotonaldehyde, could be generated in the renal proximal tubules of rats exposed to oxidative stress induced by Fe^{3+}-NTA and that they subsequently react with cytoplasmic proteins to accumulate as protein-bound aldehydes that can be recognized by mAb82D3 (Fig. 9). As far as we know, this is the first report of the *in vivo* formation of protein-bound crotonaldehyde/2-alkenals in the target organ of the carcinogenic protocol. It was also striking that the immunoreactivities with mAb82D3 were detected even 48 h after the administration of Fe^{3+}-NTA (Fig. 9*C*). Long retention of this mutagenic aldehyde may have a role in the Fe^{3+}-NTA-induced carcinogenesis.

It is of interest to note that the high molecular weight proteins that cross-reacted strongly with mAb82D3 were detected in the protein (BSA) treated with crotonaldehyde (Figs. 8*C*) and iron/ascorbate/α-linolenic acid (Fig. 10*B*). Because their molecular sizes are about 100 kDa and >200 kDa (Fig. 8*C*) and >200 kDa, it is unlikely that they are originated from the polymerization of BSA. Although the source of these proteins is currently unknown, these results invite speculation that they could be critical targets of crotonaldehyde or, to the contrary, that they may be specific scavengers of this aldehyde. Clearly, the identification of these proteins and determination of the biological consequences of their interaction with crotonaldehyde merit immediate attention.

In summary, we have characterized the reaction of protein with crotonaldehyde and determined the structures of the crotonaldehyde-amino acid adducts possessing a carbonyl function. In addition, we have obtained a new murine monoclonal antibody, mAb82D3, that clearly distinguished the crotonaldehyde-modified protein from the native protein. It appears that the antibody is specific to the pyridinium-type lysine adduct, EMP-lysine. Using this antibody, it was revealed that a single intraperitoneal treatment of rats with Fe^{3+}-NTA induced accumulation of protein-bound 2-alkenals in the renal proximal tubules, the target cells of this carcinogenesis model. In addition, the presence of antigenic materials has also been observed in the neurons of patients with amyotrophic lateral sclerosis, in which oxidative stress has been implicated as the major contributor to neuronal cell death. These data suggest that the formation of carcinogenic aldehydes during lipid peroxidation may be causally involved in the pathophysiological effects associated with oxidative stress.

REFERENCES

1. Stadtman, E. R. (1986) *Trends Biochem. Sci.* **11**, 11–12
2. Stadtman, E. R. (1990) *Free Radic. Biol. Med.* **9**, 315–325
3. Stadtman, E. R. (1992) *Science* **257**, 1220–1224
4. Stadtman, E. R., and Oliver, C. N. (1991) *J. Biol. Chem.* **266**, 2005–2008
5. Esterbauer, H., Schaur, R. J., and Zollner, H. (1991) *Free Radic. Biol. Med.* **11**, 81–128
6. Uchida, K. (2000) *Free Radic. Biol. Med.* **28**, 1685–1696
7. Steinberg, D., Parthasarathy, S., Carew, T. E., Khoo, J. C., and Witztum, J. L. (1989) *N. Engl. J. Med.* **320**, 915–924
8. Steinberg, D. (1995) *Adv. Exp. Med. Biol.* **369**, 39–48
9. International Agency for Research on Cancer (1995) *IARC Monographs on the Evaluation of Carcinogenic Risks to Humans. Dry Cleaning, Some Chlorinated Solvents and other Industrial Chemicals*, Vol. 63, pp. 373–391, International Agency for Research on Cancer, Lyon, France
10. Chung, F.-L., Tanaka, T., and Hecht, S. S. (1986) *Cancer Res.* **46**, 1285–1289
11. Chung, F.-L., Chen, H.-J. C., and Nath, R. G. (1996) *Carcinogenesis* **17**, 2105–2111
12. Chung, F.-L., Nath, R. G., Nagao, M., Nishikawa, A., Zhou, G.-D., and Randerath, K. (1999) *Mutat. Res.* **424**, 71–81
13. Wang, M., Chung, F.-L., and Hecht, S. S. (1988) *Chem. Res. Toxicol.* **1**, 28–31
14. Wang, M., McIntee, E. J., Cheng, G., Shi, Y., Villalta, P. W., and Hecht, S. S. (2000) *Chem. Res. Toxicol.* **13**, 1065–1074
15. Levine, R. L., Williams, J. A., Stadtman, E. R., and Shacter, E. (1994) *Methods Enzymol.* **233**, 346–357
16. Uchida, K., Szweda, L. I., Chae, H. Z., and Stadtman, E. R. (1993) *Proc. Natl.*

Acad. Sci. U. S. A. **90**, 8742–8746
17. Laemmli, U. K. (1970) *Nature* **227**, 680–685
18. Toyokuni, S., Uchida, K., Okamoto, K., Hattori-Nakakuki, Y., Hiai, H., and Stadtman, E. R. (1994) *Proc. Natl. Acad. Sci. U. S. A.* **91**, 2616–2620
19. Toyokuni, S., Tanaka, T., Hattori, Y., Nishiyama, Y., Yoshida, A., Uchida, K., Hiai, H., Ochi, H., and Osawa, T. (1997) *Lab. Invest.* **76**, 365–374
20. Nadkarni, D. V., and Sayre, L. M. (1995) *Chem. Res. Toxicol.* **8**, 284–291
21. Uchida, K., Kanematsu, M., Morimitsu, Y., Osawa, T., Noguchi, N., and Niki, E. (1998) *J. Biol. Chem.* **273**, 16058–16066
22. Ebina, Y., Okada, S., Hamazaki, S., Ogino, F., Li, J.-L., and Midorikawa, O. (1986) *J. Natl. Cancer Inst.* **76**, 107–113
23. Li, J.-L., Okada, S., Hamazaki, S., Ebina, Y., and Midorikawa, O. (1987) *Cancer Res.* **47**, 1867–1869
24. Toyokuni, S., Okada, S., Hamazaki, S., Minamiyama, Y., Yamada, Y., Liang, P., Fukunaga, Y., and Midorikawa, O. (1990) *Cancer Res.* **50**, 5574–5580
25. Uchida, K., Fukuda, A., Kawakishi, S., Hiai, H., and Toyokuni, S. (1995) *Arch. Biochem. Biophys.* **317**, 405–411
26. Sohal, R. S., Agarwal, S., Dubey, A., and Orr, W. C. (1993) *Proc. Natl. Acad. Sci. U. S. A* **90**, 7255–7259
27. Smith, C. D., Carney, J. M., Starke-Reed, P. E., Oliver, C. N., Stadtman, E. R., Floyd, R. A., and Markesbery, W. R. (1991) *Proc. Natl. Acad. Sci. U. S. A.* **88**, 10540–10543
28. Oliver, C. N., Ahn, B.-W., Moerman, E. J., Goldstein, S., and Stadtman, E. R. (1987) *J. Biol. Chem.* **262**, 5488–5491
29. Bowling, A. C., Schultz, J. B., Brown, R. H., Jr., and Beal, M. F. (1993) *J. Neurochem.* **61**, 2322–2325
30. Gladstone, I. M., and Levine, R. L. (1994) *Pediatrics* **93**, 764–768
31. Berlett, B. S., and Stadtman, E. R. (1997) *J. Biol. Chem.* **272**, 20313–20316
32. Uchida, K., and Stadtman, E. R. (1993) *J. Biol. Chem.* **268**, 6388–6393
33. Burcham, P. C., and Kuhan, Y. T. (1996) *Biochem. Biophys. Res. Commun.* **220**, 996–1001
34. Esterbauer, H., Ertl, A., and Scholz, N. (1976) *Tetrahedron* **32**, 285–289
35. Alaiz, M., and Barragán, S. (1995) *Chem. Phys. Lipids* **75**, 43–49
36. Baker, A., Zídek, L., Wiesler, D., Chmelík, J., Pagel, M., and Novotny, M. V. (1998) *Chem. Res. Toxicol.* **11**, 730–740
37. Baker, A., Wiesler, D., and Novotny, M. V. (1999) *J. Am. Soc. Mass. Spectrom.* **10**, 613–624
38. Awai, M., Narasaki, M., Yamanoi, Y., and Seno, S. (1979) *Am. J. Pathol.* **95**, 663–674
39. Toyokuni, S. (1996) *Free Radic. Biol. Med.* **20**, 553–566